JOURNAL OF ENGINEERING AND APPLIED SCIENCE, VOL. 51, NO. 1, FEB. 2004, PP. 139-156
FACULTY OF ENGINEERING, CAIRO UNIVERSITY

COMPUTER MODELING OF SUSCEPTIBILITY CONTRAST MECHANISMS IN MAGNETIC RESONANCE IMAGING

N. El-SHABRAWY[1], A. S. MOHAMED[2], A. YOUSSEF[3], AND Y. M. KADAH[4]

ABSTRACT

Among the unique features of magnetic resonance imaging (MRI) is the ability to image physiological function and chemical composition besides anatomy non-invasively. In functional brain MRI, it is possible to map the area of the brain that is activated under a particular mental, sensory, or motor task provided by the physician. This allows the identification of brain centers and opens the door for scientists to understand the complex mechanisms inside the human nervous system. Even though the experimental techniques that enable the mapping of function have been established in the last decade, the underlying contrast mechanisms are still not fully understood. In this work, we propose a general model to the process of contrast generation in MRI based on Monte Carlo simulations. The proposed model allows researchers to test hypotheses about the contrast in a particular setting as well as to study the effect of different pulse sequences on the process of functional imaging. The proposed model is described in detail and validated using experimental data from the literature. Then, it is applied to explain other problems in functional MRI. The results demonstrate the value of the model in allowing researchers to better understand contrast mechanisms.

KEYWORDS: Magnetic Resonance Imaging, Contrast Agents, Susceptibility, Monte Carlo, Modeling, Functional Imaging, T_2* contrast.

1. INTRODUCTION

When evaluating suitable enhancement agents in magnetic resonance imaging, their magnetic susceptibility is an important parameter to consider [1]. Magnetic susceptibility is a fundamental property of matter and it defines the ability of the external magnetic field to affect the nuclear precession of a spin [2]. Among the most

[1] Graduate Student, Systems and Biomedical Dept., Faculty of Engineering, Cairo University, Egypt.
[2] Lecturer, Systems and Biomedical Dept., Faculty of Engineering, Cairo University, Egypt.
[3] Professor, Systems and Biomedical Dept., Faculty of Engineering, Cairo University, Egypt.
[4] Associate Professor, Systems and Biomedical Dept., Faculty of Engineering, Cairo University, Egypt.

common encounters of such effects is in the diamagnetic and paramagnetic changes of the blood. This is determined by the balance between the paramagnetic oxyhemoglobin and the diamagnetic deoxyhemoglobin at any given time, which determines the T_2 and T_2^* characteristics of the sample [2-3]. Given that the paramagnetic oxyhemoglobin appears brighter than the diamagnetic deoxyhemoglobin on T_2- or T_2^*- weighted MRI images, the difference in signal between different states has been used to identify the activated areas inside the brain [4-5]. In cases of pathological conditions such as intra-cranial lesions, localization becomes even more difficult when the lesion invades eloquent brain regions and distorts structural landmarks and functional locations. In many cases, pre-surgical localization of brain function can identify eloquent cortex to reduce postoperative complications, yet allows removal of the diseased tissue. Therefore, MRI techniques with the ability to assess the functionality of brain regions provide vital information in cases of distorted brain anatomy and neurological disorders, as well as aid in the understanding of normal brain processing [2-3].

Given its important applications in medicine, several studies have been conducted to identify and explain the susceptibility-based contrast mechanisms in MRI. Kennan, et al. [6] studied the intravascular susceptibility contrast mechanisms in tissues where the factors affecting the rate of transverse relaxation in gradient echo and spin-echo pulse sequences have been quantified using computer modeling of media containing arrays of susceptibility variation. The results are particularly relevant for describing the signal loss in tissues containing capillaries of altered intrinsic susceptibility as a result of administration of exogenous contrast agent or changes in blood oxygenation level. Several groups studied the microscopic susceptibility variation and transverse relaxation theory and found experimentally that microscopic susceptibility variations invariably increase apparent transverse relaxation rates [7-9]. They presented comparisons between Monte Carlo simulations and experiments with polystyrene micro-spheres to demonstrate that this enhanced relaxation can be explained quantitatively for both spin echo and gradient echo imaging experiments. The sphere sizes and the degree of susceptibility variation covered a wide range of

biologically relevant compartment sizes and contrast agent concentrations. The results showed that several regimes of behavior existed, and that contrast dependence was quite different in those regimes. They found that susceptibility induced relaxation rates that vary approximately linearly with concentrations of injected contrast agents. Even though this model met a wide acceptance in the academic community, it lacked the flexibility to include more general experimental situations.

To illustrate the need for a more flexible tool for simulating susceptibility contrast mechanisms, we consider the debate about the paper by Menon *et al.* [10] where the scientific community split over the possibility of achieving their break-through results. In this work, they studied sub-millimeter functional localization in human striate cortex using blood oxygenation level dependent (BOLD) contrast at 4 Tesla and its implications for the vascular point-spread function [8]. Using visual stimulation in a feline model in which a 1×1 mm patch of cortex demonstrated spiking neurons. They claimed to be able to outline the form of the ocular dominance column corresponding to each eye in the primary visual cortex. This was previously only possible using optical imaging. The reason why this study generated a lot of debate in the scientific community was the stringent requirements imposed on the spatial and temporal resolution of the imaging involved, which push the physics to near its fundamental limits. Therefore, a model that allows the simulation of the experimental settings would be very useful for objective assessment the results of such research.

In this work, we propose a general numerical model for the process of susceptibility contrast generation in functional MRI (fMRI). This model was built to allow more flexibility than previous models such that various experimental situations can be simulated. In particular, effect of perturber movement and the presence of red blood cells (RBCs) are taken into account. The model studies the signal changes due to arbitrary contrast mechanisms based on the Monte Carlo method. The objective is to allow the study of applications involving contrast mechanisms and applications including BOLD contrast, as well as vessel contrast in magnetic resonance angiography using Gadolinium-Chelate (Gd-DTPA or in short Gd here) and Dysprosium-Chelate (Dy-DTPA or in short Dy here) [2-3]. The developed model is

validated using three independent experimental data sets cited in the literature and then applied to explain two problems in fMRI. The proposed model can be useful for researchers to understand and develop new contrast mechanisms as well as an educational tool for students and physicians.

The rest of this paper is composed of five sections. In section 2, we describe the modeling and simulation method and then provide the implementation steps used to generate the results of this paper. In section 3, we describe the methodology for model verification. In section 4, we present the results of this work followed by a discussion in section 5 and conclusions in section 6.

2. MODELING AND SIMULATION METHOD

The simulation of proton random walks to estimate transverse magnetization variation with different contrast parameters in the presence of inhomogeneous magnetic field is performed using Monte Carlo methods [11]. In particular, we compute the magnetic resonance signal *S(t)* corresponding the transverse magnetization based on the complex sum of the spin signals. Here, the signal from each spin is assumed to have a unit magnitude with a random phase and the expectation operator is applied over the initial position of the protons as well as for each possible position along its random walk through the medium. The Monte Carlo methods are used to compute the resultant signal from *N* randomly distributed protons such that [7],

$$S(t) = \sum_{n=1}^{N} e^{j\phi_n(t)} , \qquad (1)$$

where $\phi_n(t)$ is the phase of the n^{th} spin at time *t*. Monte Carlo estimation is actually used to calculate the sum over starting locations and as the stochastic walk of the protons produces phases that are uniformly distributed. The steps to produce a Monte Carlo estimate of the change in imaging relaxation rate, R_2^* are:

1- Distribute *n* impenetrable spherical perturbers randomly throughout a prescribed region (i.e., cylindrical sub-compartment to simulate a capillary or venule).
2- Distribute *N* protons throughout a prescribed region (for example region of interest in tissue as $L\times L\times L$ voxel).
3- For every time step Δt, simulate the stochastic diffusion of the protons and perturbers by choosing a random displacement (with zero mean and standard deviation $\delta r = \sqrt{6D\Delta t}$, where *D* is the diffusion coefficient) in the *x*, *y* and *z* directions. This is different from [7-9] in which protons only move.
4- Evaluate the magnetic field at the proton's new location by summing the fields from all perturbers assuming that the cylindrical capillary volume contains a uniformly distributed paramagnetic agent. For the case of a spherical particle, the magnetic field perturbation takes the form [6-9],

$$\frac{\Delta B_z(r,\theta)}{B_o} = \frac{4\pi}{3}\Delta\chi(\frac{R}{r})^3(3\cos^2\theta - 1) \qquad (2)$$

where *r* and θ are the usual spherical coordinates, *R* is the radius of the sphere, and $\Delta\chi$ is the magnitude of the susceptibility difference between the sphere and the surrounding medium and its value changed according to the type of the contrast agents. The value of $\Delta\chi$ for Gd is 2.55×10^{-2} ppm, for Dy is 3.55×10^{-2} ppm, while that of deoxyhemoglobin is 8×10^{-2} ppm taken at B_0 of 2 Tesla. The size of this universe depends on the diffusion coefficient, the maximum echo time (TE), and the size of the spheres. Alternatively, when the cylindrical capillary volume contains a uniformly distributed paramagnetic agent the interior possesses uniform magnetization per unit volume but the susceptibility difference between the intra- and extra-vascular spaces generates a field perturbation $\Delta B_z(r)$ throughout the extra-vascular region which has a component in the direction of the external field (taken to be in the *z* direction) given by [6-9]:

$$\frac{\Delta B_z(r,\phi)}{B_o} = \Delta\chi\left(\frac{4\pi R_c^2.\cos(2\phi).\sin^2(\alpha)}{2r^2}\right) \quad (3)$$

where $\Delta\chi$ is the magnetic susceptibility difference of the agent, R_c is the radius of the capillary, r and ϕ are the usual cylindrical coordinates, and α is the angle between the primary magnetic field B_0 and the axis of the capillary. Unless otherwise stated we shall generally give results for the case of the main field being perpendicular to the capillary; i.e., $\alpha = \pi/2$. For linear magnetic materials the effective magnetization can be written in terms of the external field and the difference in the volume magnetic susceptibilities between the extra and intra-capillary space, Δx_v, as: $M = \Delta x_v B_0$.

5- Evaluate the accumulated phase by numerical integration where,

$$\Delta\phi = \gamma.\Delta B_z.\Delta t \quad (4)$$

Here γ denotes the proton gyromagnetic constant, and ΔB_z is the component of magnetic field induced by perturbers as given by Eq. (2) or induced by the capillary as given by Eq. (3) at the particular proton location.

6- Steps 3-5 were repeated N times to calculate the phase of N protons, recorded at Δt time step for each.

7- The estimate for the signal was produced from the phases of the individual protons by Eq. (1). The phase for each proton is computed as the accumulation of phases in all steps Δt until acquisition TE. For example, assuming 6 Δt steps, the total phase for a gradient echo sequence [12] at TE = 6Δt, is $\sum_{m=1}^{6}\phi_{n,m}$ while the phase for spin echo [12] is $\sum_{m=1}^{3}\phi_{n,m}$ - $\sum_{m=4}^{6}\phi_{n,m}$, where $\phi_{n,m}$ is the phase of spin n at time $m\ \Delta t$.

3. MODEL VERIFICATION

3.1 Effect of Different Types of Contrast Agents on Signal Intensity

Here, we study the effect of different types of contrast agents, either chemical or intrinsic on signal intensity as well as relaxation rates. Simulations used 10,000 protons, walking in Δt = 1ms time steps during echo times of 6 to 61ms. The diffusion coefficient was set to 1.3×10^{-5} cm^2/s, which corresponds to the water diffusion coefficient for the experimental conditions. Our results shown in Fig. 1 indicate that the paramagnetic contrast agents Dy, Gd and deoxyhemoglobin function by shortening the T_2 of nearby water protons decreasing signal intensity. A decrease in tissue signals intensities are observed in Fig. 2 with the fact that Dy signal decrease is substantially greater in degree than that observed with equivalent Gd. As paramagnetic agents initially pass through the vascular bed of the brain, of course deoxyhemoglobin decrease signal is the greatest in degree comparing to the others (Gd and Dy) and this results were expected as the higher susceptibility degree varies with the following order deoxyhemoglobin 8×10^{-2} ppm, Dy 3.5×10^{-2} ppm, Gd 2.5×10^{-2} ppm. The final conclusion from our simulation results shown in Figs. 1-3 indicates that Dy would be more effective than Gd in T_2^* weighted images due to its highly susceptibility. The results agree with the experimental relaxation rate enhancement as a function of intravascular concentration for Gd and Dy [7-9].

3.2 Effect of Contrast Agent Distribution in Tissue

Here the proposed model is utilized to study the effect of the distribution of susceptibility based contrast agent in tissue on the echo signals. The simulation was performed on two types of contrast agent distributions. The results are shown in Fig. 4. The first contrast agent, designated with symbol '*', represents a uniformly distributed agent whereby the magnetic field within this space is uniform. On the other hand, the second contrast agent, designated with symbol 'o', is for the same amount of agent

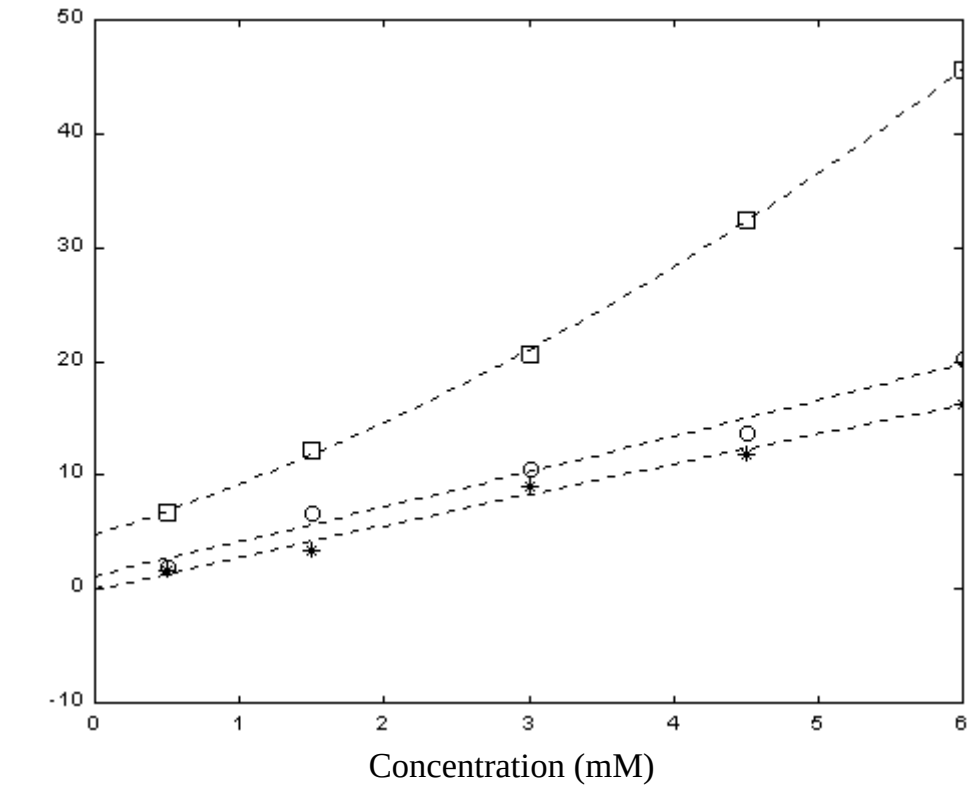

Fig. 1. Comparison of Gd (*), Dy (o) and deoxyhemoglobin (2R setar noitaxaler (ف*
(Concentration in mMolar (mM)).

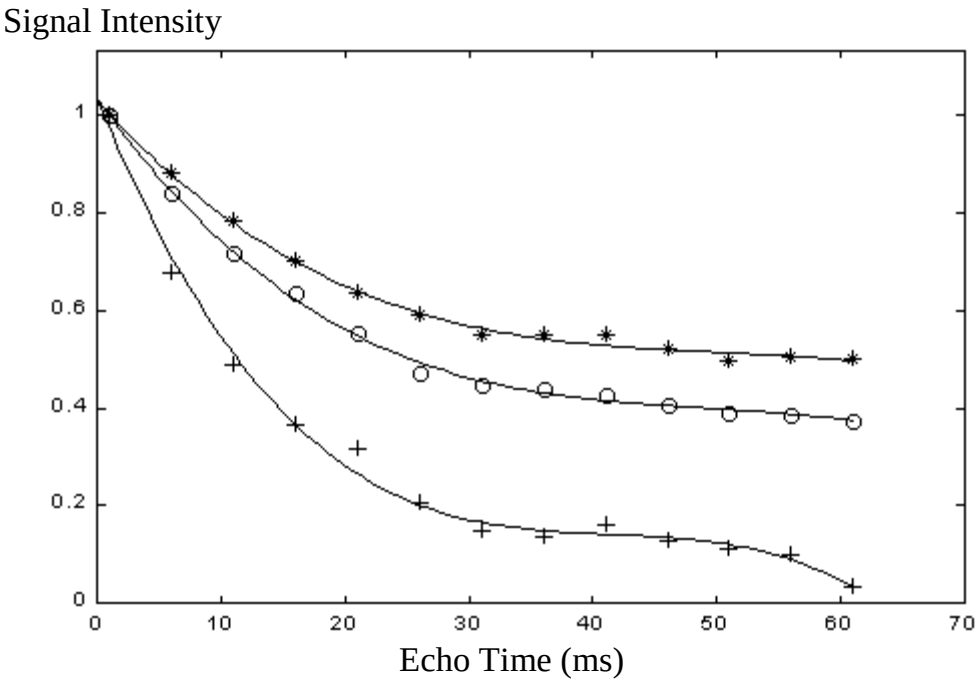

Fig. 2. Comparison of Gd (*), Dy (o) and deoxyhemoglobin (+) signal intensities.

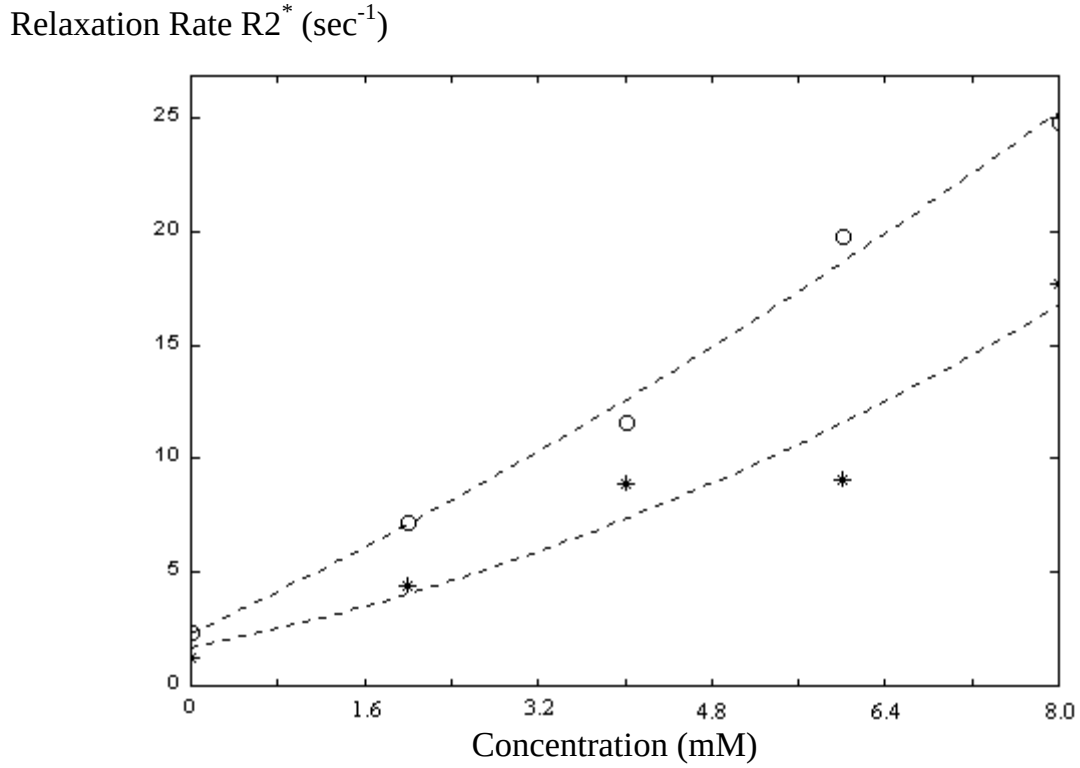

Fig. 3. Gd (*) and Dy (o) relaxation rates versus concentration.

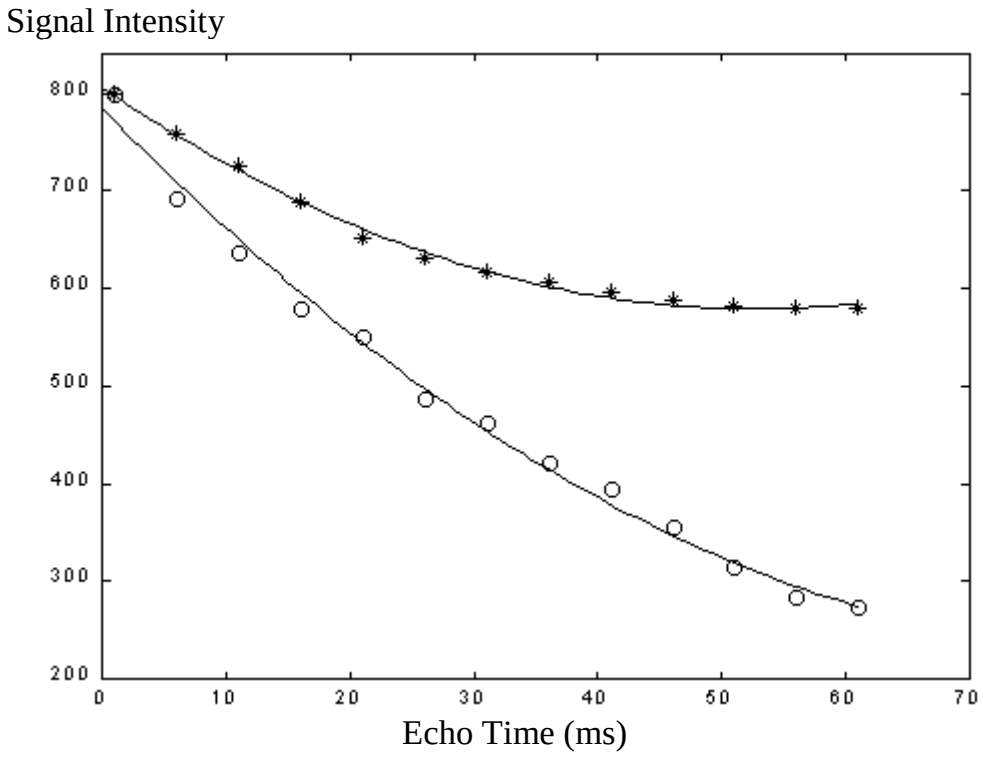

Fig. 4. Effect of the distribution of a susceptibility based contrast agent in tissue ('*' uniform distribution, 'o' subcompartment nonuniform distribution).

within compartments whereby a non-uniform field distribution throughout the region is generated. Simulations used 10000 protons, walking in Δt = 1ms time steps during echo times of 6 to 61 ms. The diffusion coefficient was set to 1.3×10^{-5} cm^2/s, which corresponds to the water diffusion coefficient for the experimental conditions. The susceptibility distribution of the sub compartments is expected to be important as shown in our results (Fig. 4). The signal intensity for sub compartment distribution is dephasing exponentially highly than the uniform distribution and this result agrees with the previous studies of susceptibility effects. Previous studies of susceptibility effects have identified distinct processes that may cause signal changes. These are illustrated in [7-9], which show two examples of the distribution of a high susceptibility agent such as a lanthanide chelate. The agent might be distributed uniformly within a pixel. In this case, the agent may relax water by paramagnetic dipolar interactions the overall bulk susceptibility increases so there is a net shift in magnetic resonance frequency, but the region is still magnetically homogeneous and there are no intrinsic field gradients or variations. If, however, the same amount to agent is distributed in multiple small sub-compartments, then several other factors become important. While water inside each sub-compartment may experience paramagnetic dipolar interactions, fraction of the whole sample that is relaxed in this way depends on the water exchange across the compartment boundaries in the time of measurement. This therefore introduces a dependence on water diffusion and boundary permeability. A second dependence on diffusion is expected because outside the sub-compartments a field perturbation is produced that is spatially nonuniform and proportional to the magnetization introduced by the agent. Random motion of the spins through these field gradients will contribute to spin dephasing. Even without motion or exchange of the spins the field pattern is nonuniform and thus nuclei will precess with a range of Larmor frequencies and over time the signal will dephase. The geometrical arrangement of the sub-compartments is expected to be important.

3.3 Effect of Gradient-Echo vs. Spin-Echo Techniques on Relaxation Rate

Our goal here is to use our model to study the effect of different types of techniques on relaxation rate and show their effectiveness in T_2^* weighted images. Fig. 5 shows the result for the simulated relaxation rate enhancement as a function of intra-vascular concentration for Dy evaluated at 85 MHZ. Simulations used 10,000 protons, walking in Δt = 1 ms time steps during echo times of 6 to 61 ms. The diffusion coefficient was set to 1.3×10^{-5} cm^2/s, which corresponds to the water diffusion coefficient for the experimental conditions with a capillary diameter of 8 μm. We can see that over the range of concentration shown (0-100 %), that the Gradient echo relaxation rate curve (represented by symbol 0) is higher than the Spin-Echo relaxation rate curve (symbol '*') so we conclude an important fact that the Gradient-echo technique would be more effective than spin-echo technique in T_2^* weighted images and this result expected as the 180^o pulse used in the spin echo technique eliminates

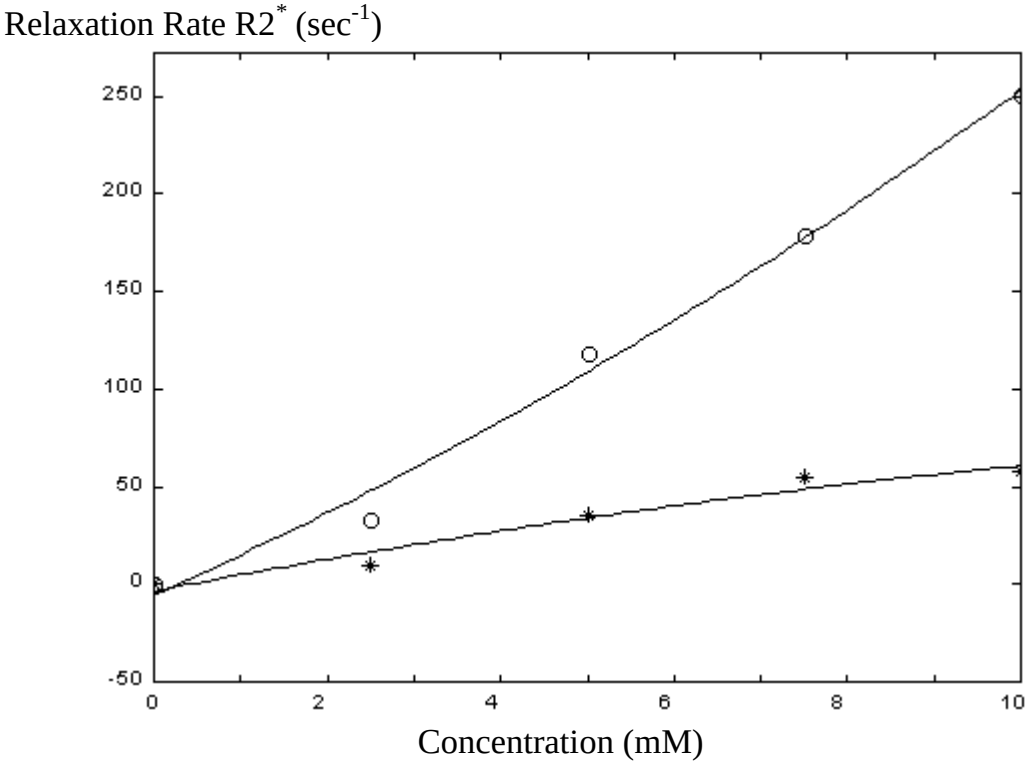

Fig. 5. Comparison of gradient-echo (o) and spin-echo (*) relaxation rates $R2^*$.

the effects of the magnetic field inhomogeneity and allows decay to be a function of spin-spin interaction only. This is a true T_2 decay. The 180^o pulse thought as a re-focusing pulse, which eliminates external artifactual causes of dephasing and allows only the tissue characteristics, i.e., internal magnetic field inhomogeneities the spin-echo technique is not effective in T_2^* weighted images as the Gradient echo technique in case of using contrast agents as the contrast agents play a very important role as a source of external artifacts. The results agree with the results obtained from the experimental relaxation rate enhancement as a function of intra-vascular concentration for Dy [7-9].

4. APPLICATIONS

4.1 Activation Detection Within the Ocular Dominance Columns

As BOLD contrast has been extensively used to non-invasively map human brain processes, ranging from sensory perception to cognitive function [10]. We have performed a computer simulation of model system for layer 4C [13] by using a model with four sub-compartments. The simulation here is aimed at verifying the physical possibility of separating activations between neighboring ocular dominance columns. This will help resolve the debate about the results published in [10]. The simulation used 10,000 protons, walking in Δt = 1 ms time steps during echo times between 6-61 ms. The diffusion coefficient was set to 1.3×10^{-5} cm^2/s, which corresponds to the water diffusion coefficient for the experimental conditions, in which an agent (deoxyhemoglobin) resides inside a certain number of sub-compartments, our model has four sub-compartments representing the four ocular dominance columns in layer 4C, our studied cases are as follows:

1- Left eye only is stimulated: In this case, we simulate an activation within the odd numbered sub-compartments representing ocular dominance columns. These columns have the advantage that they can be selectively and noninvasively activated using photic stimulation of one eye (independent of stimulus size in degrees). As the result, the physiological response of sub-compartments 1 and 3 to

increases in regional blood volume and flow gives rise to a decrease in the local concentration of deoxyhemoglobin. The loss of paramagnetic deoxyhemoglobin from sub-compartments is thought to make the cell tissue more magnetically homogeneous so that signal intensity increase., as shown in our result in Fig. 6 for first and third columns, the signals obtained are high. Meanwhile, within the even sub-compartments, the level of local concentration of deoxyhemoglobin remains at the same level of concentration in which the cell tissue magnetically inhomogeneous state so the signal intensity decreases as shown in Fig. 6 for second and fourth columns, where the signals obtained are low.

2- Right eye only is stimulated: This is exactly the opposite of the case discussed above where the even columns here provide a higher signal. The simulation of this case is shown in Fig. 7.

3- No stimulation: Here, the case when no stimulation of both odd and even ocular dominance columns is simulated. The signal intensities from both compartments were found to be low.

4- Both eyes are stimulated: Here, we simulate an activation of both odd and even ocular dominance columns using photic stimulation applied for both left and right eyes. Here, the signals intensities obtained are all high.

Hence, the results of our simulation indicate that even though the sub-compartments representing the ocular dominance columns are very small in size, it is still possible to discern the signals difference between even and odd columns. This result supports the hypothesis that the results in [10] are possible to obtain.

4.2 Diffusion Process Simulation

In some special magnetic resonance imaging applications, the contrast agent is injected and left until it washes out before imaging starts. This uses what is called post-contrast enhancement principle to image the walls of vessels and assess their viability. This principle is based on the diffusion of contrast agent in the vessel walls.

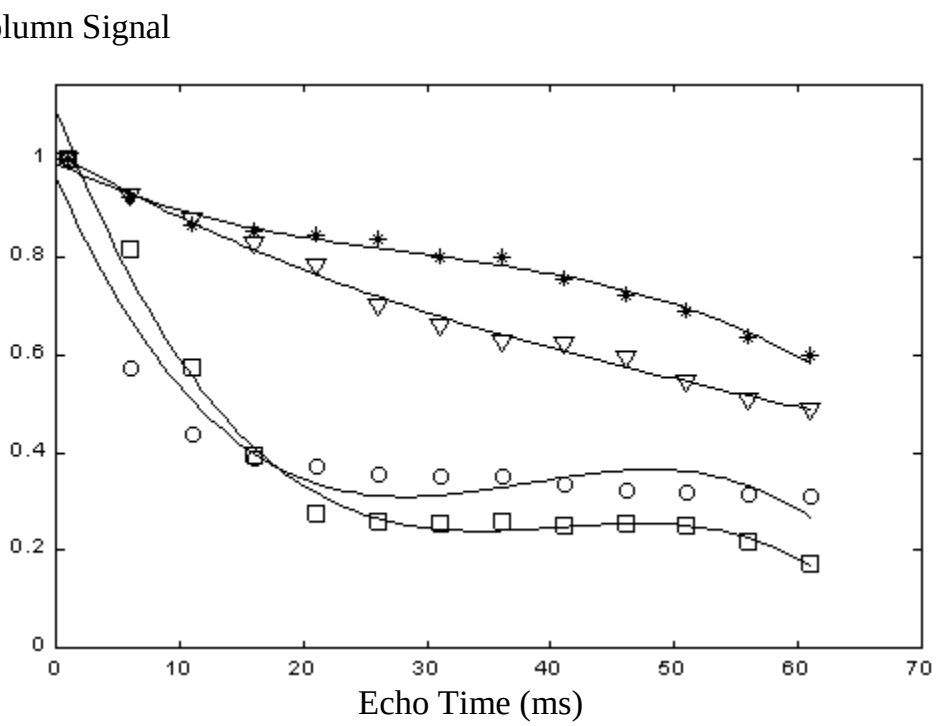

Fig. 6. Case of left eye simulated (‘*’ 1st column, ‘o’ 2nd column, ‘triangle’ 3rd column, ‘ڤ’ 4th column).

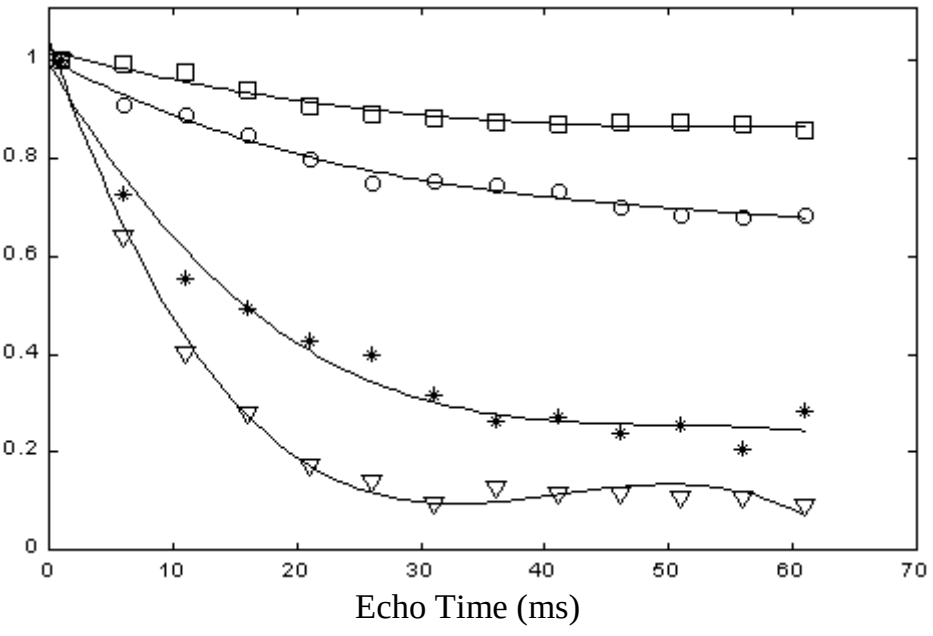

Fig. 7. Case of right eye simulated (‘*’ 1st column, ‘o’ 2nd column, ‘triangle’ 3rd column, ‘ڤ’ 4th column).

Here, we present a simulation of this diffusion process. Our simulation results shown in Fig. 8 where we simulate diffusion as in the case of semi-permeable membrane with a constant contrast agent inside the vessel maintained at the same level (i.e., echo signals taken during the first time of the agent bolus). Simulations used 10,000 protons, walking in Δt = 1ms time steps during echo times of 6 to 61ms. The diffusion coefficient was set to 1.3×10^{-5} cm^2/s, which corresponds to the water diffusion coefficient for the experimental conditions. Fig. 8-a shows that the signal intensity is decayed with a nice exponential curve. In Fig. 8-b, the contrast agent concentration inside the capillary is presented with the symbol '*' and outside the capillary is presented with the symbol 'o'. As we see, the contrast agent concentration inside the capillary is constant while the concentration outside is increasing due to the diffusion effect that diffuse the perturbers from inside to outside the capillary through the semi permeable membrane which represent the normal case in order to reach the equilibrium state where both the concentration inside and outside is equal. The diffusion flux is plotted against the echo time (Fig. 8-c) and it is clear that the flux is decayed till it reaches zero where equilibrium state occurred. This simulation can be used to find out the optimal time to acquire images after injecting the contrast agent at a given concentration. This can be performed for any new contrast agent. It can also be used as an educational tool to help physicians better understand this principle.

5. DISCUSSION

We have demonstrated that Monte Carlo modeling of microscopic susceptibility variation produces excellent predictions of apparent T_2^* relaxation. The results presented here accord closely with the results reported by literature. The developed numerical model is useful in designing of experimental magnetic resonance imaging sequences, contrast agents, as well for educational purposes. Several factors have considered which are important for a quantitative understanding of susceptibility induced signal losses in tissue. It is clear that susceptibility based relaxation is strongly dependent on magnetic, geometric, and dynamic properties of the tissue. Further

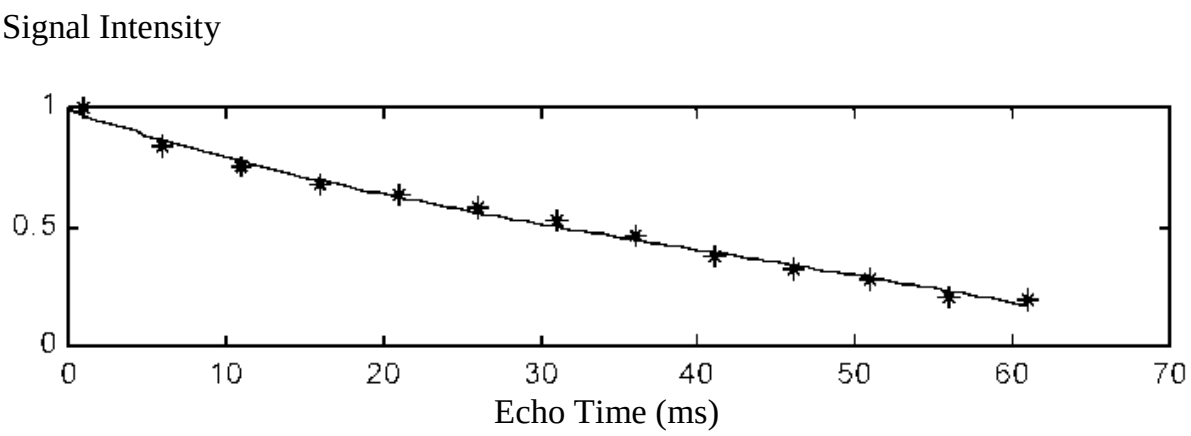

(a)

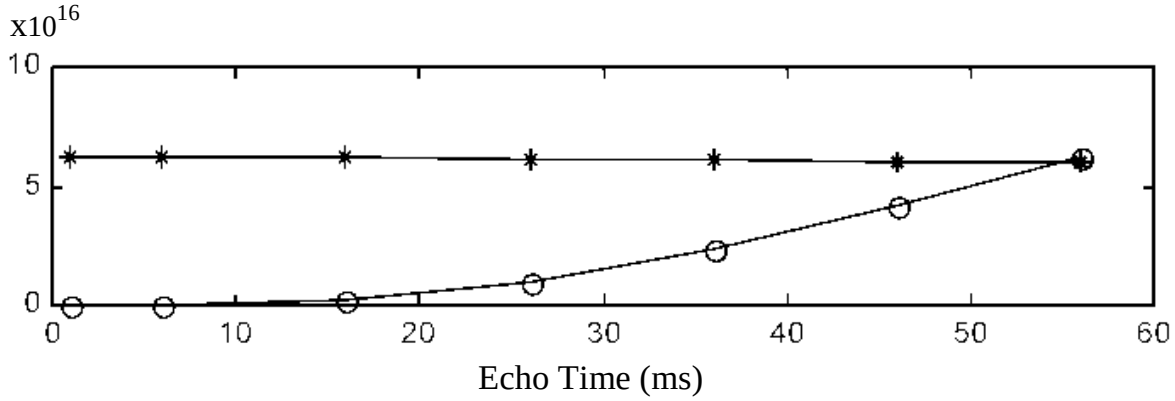

(b)

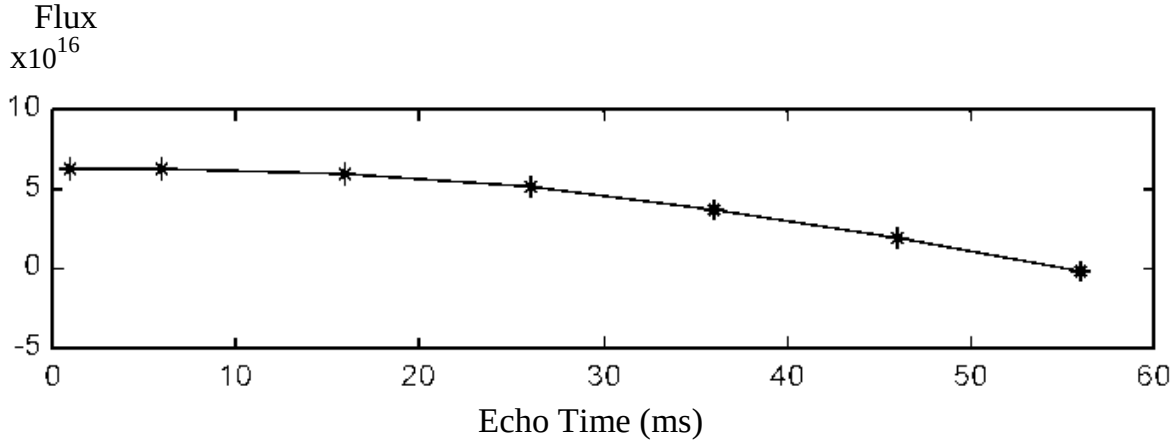

(c)

Fig. 8. Simulation of diffusion (case constant contrast agent concentration). (a) Signal intensity versus echo time. (b) Perturbers concentration versus echo time ('*' concentration inside capillary and 'o' concentration outside capillary). (c) The flux versus echo time.

understanding of this dependence may have important consequent for the choice of field, design of pulse sequences, and the design of magnetic contrast agents for MRI. From computer simulations we have found that, the highest level of transverse relaxation will be achieved by small perturber diameter compared to large diameter. The greatest relaxation effects are expected from distributions of larger vessels such as arterioles and venules (particularly the dependence of different relaxation rates on vessel size and position). Use exogenous contrast agents in order to enhance signal effects from capillaries. If vasodilatation occurs, the resultant change in relaxation rate is much greater than if vessels recruitment occurs. The loss of paramagnetic deoxyhemoglobin from sub-compartments is thought to make the cell tissue more magnetically homogeneous so that signal intensity increased. Susceptibility induced signal losses in tissue tend to show much greater dependence on geometry, numbers of capillaries.

6. CONCLUSIONS

A computer model was developed to study the effect of susceptibility-based contrast in magnetic resonance imaging. The model allows the simulation of various contrast imaging situations with high degree of flexibility. The model was verified using published experimental data from three different applications. Then, it was used to explain the experimental results in two other applications. The model has a large potential for educational purposes as well as to help researchers design suitable imaging protocols for new contrast imaging applications.

REFERENCES

1. D.D. Stark and W.G. Bradley, Magnetic Resonance Imaging, 3rd ed., Mosby, Inc., New York, 1999.
2. G.K. Van Schulthess and J. Hennig, Functional Imaging, Lippincott-Raver, New York, 1997.
3. W.W. Orrison, J.D. Lewine, J.A. Sanders and M.F. Hartshorne Functional Brain Imaging, Mosby, New York, 1995.

4. S. Ogawa, R.S. Menon, D.W. Tank, S.-G. Kim, H. Merkle, J.M. Ellermann and K. Ugurbil, "Functional brain mapping by blood oxygenation level-dependent contrast magnetic resonance imaging," Biophys. J., vol. 64, pp. 803-812, 1993.
5. T.Q. Duong, D.-S. Kim, K. Ugurbil, and S.-G. Kim "Spatiotemporal dynamics of the BOLD fMRI signals: toward mapping submillimeter cortical columns using the early negative response," Magn. Reson. Med., vol. 44, pp. 231-242, 2000.
6. R.P. Kennan, J. Zhong and J.C. Gore, "Intravascular susceptibility contrast mechanisms in tissues," Magn. Reson. Med., vol. 31, pp. 9-21, 1994.
7. R.M. Weisskoff, C.S. Zuo, J.L. Boxerman and B.R. Rosen, "Microscopic susceptibility variation and transverse relaxation: theory and experiment," Magn. Reson. Med., vol. 31, pp. 601-610, 1994.
8. J.L. Boxerman, L.M. Hamberg, B.R. Rosen and R.M. Weisskoff, "MR contrast due to intravascular magnetic susceptibility perturbations," Magn. Reson. Med., vol. 34, pp. 555-566, 1995.
9. D.A. Yablonsky and E.M. Haacke "Theory of NMR signal behavior in magnetically inhomogeneous tissue: the static dephasing regime," Magn. Reson. Med., vol. 32, pp. 749-763, 1994.
10. R.S. Menon and B.G. Goodyear, "Submillimeter functional localization in human striate cortex using BOLD contrast at 4 Tesla: implications for the vascular point-spread function," Magn. Reson. Med., vol. 41, pp. 230-235, 1999.
11. M.H. Kalos and P.A. Whitlock, Monte Carlo Methods, Part 1, John Wiley & Sons, New York, 1986.
12. E.M. Haacke, R.W. Brown, M.R. Thompson and R. Venkatesan, Magnetic Resonance Imaging: Physical Principles and Sequence Design, John Wiley & Sons, New York, 1999.
13. A.C. Guyton, Textbook of Medical Physiology, 7th ed., W.B. Saunders Company, Philadelphia, 1986.

نمذجة تاثير تقنية تباين صورة الرنين المغناطيسى

فى البحث تم اقتراح نموذج عام لعملية احداث التباين فى التصوير بالرنين المغناطيسى مرتكزا على المحاكة بطريقة مونت كارلو وهذا النموذج يسمح للباحثين باختبار الافتراضات عن التابين فى الظروف المختلفة كما يمكن دراسة تاثير الاساليب المختلفة للتصوير الوظيفى للمخ، وقد شرح النموذج المقترح بالتفصيل وتم أختبار صحته باستخدام نتائج معملية من المراجع وتم تطبيق هذا النموذج لتوضيح مشاكل أخرى فى التصوير للمخ باستخدام الرنين المغناطيسى ولقد أظهرت النتائج أهمية النموذج فى السماح للباحثين لفهم أفضل لتقنية التباين.